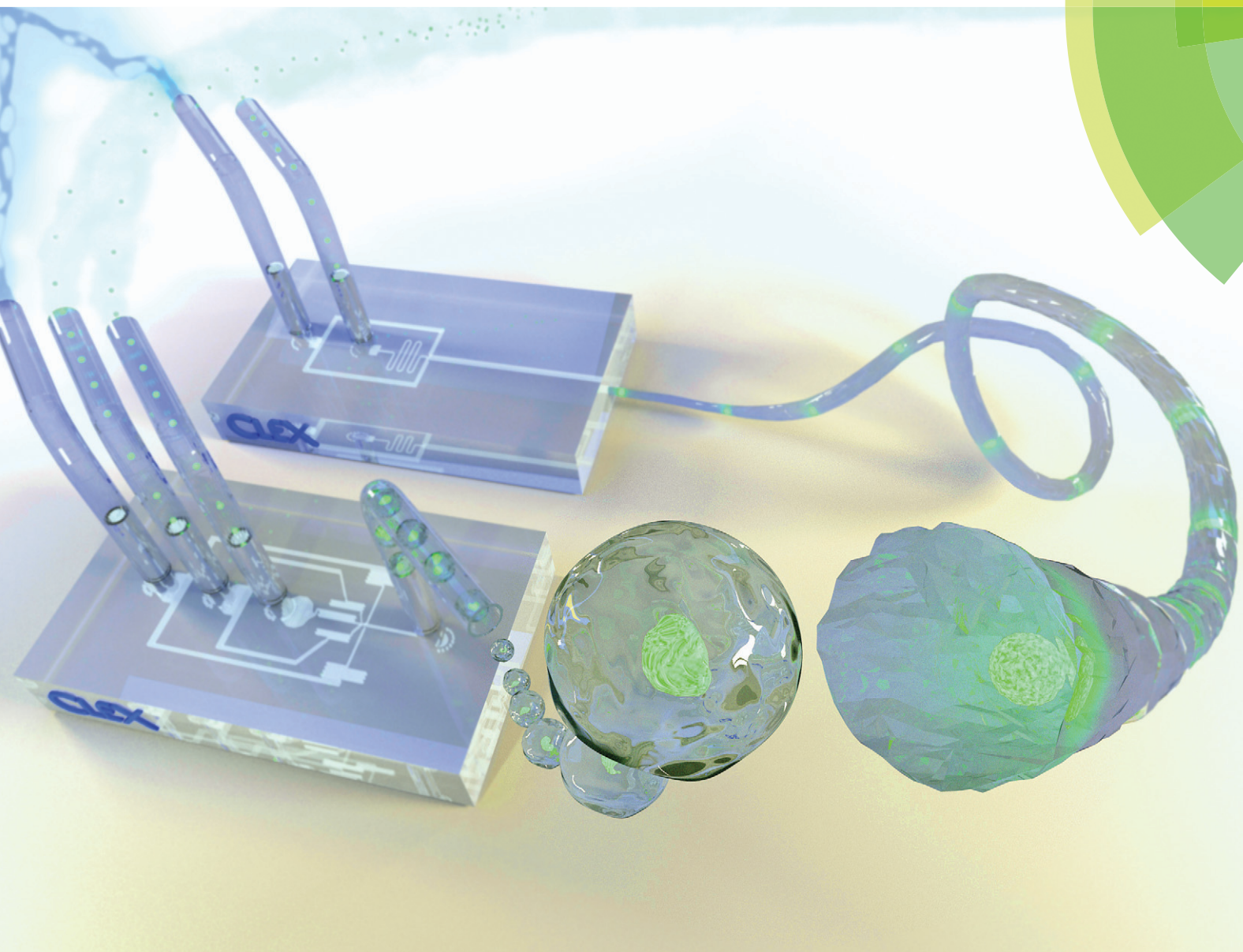


# Lab on a Chip

Miniaturisation for chemistry, physics, biology, materials science and bioengineering

[www.rsc.org/loc](http://www.rsc.org/loc)



ISSN 1473-0197



**PAPER**

Bjørn T. Stokke *et al.*  
Versatile, cell and chip friendly method to gel alginate in microfluidic devices

**175** YEARS



## Versatile, cell and chip friendly method to gel alginate in microfluidic devices†

Armend G. Håti,<sup>‡a</sup> David C. Bassett,<sup>‡a</sup> Jonas M. Ribe,<sup>a</sup> Pawel Sikorski,<sup>a</sup>  
 David A. Weitz<sup>b</sup> and Bjørn T. Stokke<sup>\*a</sup>

Cite this: *Lab Chip*, 2016, 16, 3718

Received 16th June 2016,  
 Accepted 10th August 2016

DOI: 10.1039/c6lc00769d

[www.rsc.org/loc](http://www.rsc.org/loc)

Alginate is used extensively in microfluidic devices to produce discrete beads or fibres at the microscale. Such structures may be used to encapsulate sensitive cargoes such as cells and biomolecules. On chip gelation of alginate represents a significant challenge since gelling kinetics or physicochemical conditions are not biocompatible. Here we present a new method that offers a hitherto unprecedented level of control over the gelling kinetics and pH applied to the encapsulation of a variety of cells in both bead and fibre geometries. This versatile approach proved straightforward to adjust to achieve appropriate solution conditions required for implementation in microfluidic devices and resulted in highly reliable device operation and very high viability of several different encapsulated cell types for prolonged periods. We believe this method offers a paradigm shift in alginate gelling technology for application in microfluidics.

## Introduction

Hydrogels are an important class of soft materials with far ranging applications in biomedicine, health, food and pharmaceutical sciences. Current strategies used to form discrete hydrogel particles or droplets include electrostatic extrusion,<sup>1,2</sup> acoustic emulsification,<sup>3</sup> microfluidic micro-nozzle array<sup>4</sup> and airflow nozzles.<sup>5</sup> However, these techniques have limitations in terms of producing small (below 100  $\mu\text{m}$ ) and monodisperse particles. To overcome these limitations, microfluidics has emerged as a powerful technique to form discrete and uniform hydrogel structures at the microscale. This technique has a particular focus on the encapsulation of high value or delicate cargoes such as antibodies,<sup>6</sup> proteins<sup>7</sup> and cells for diagnosis and drug development,<sup>8,9</sup> for example. Additionally, microfluidics supports the production of multicomponent structures such as core-shell or Janus particles by combination of hydrogel forming polymers and aqueous solutions from discrete flows.<sup>10</sup> From a vast library of hydrogel forming (bio)polymers, alginate, a linear polysaccharide comprised of combinations of  $\beta$ -D-mannuronic (M) and  $\alpha$ -L-guluronic (G) acid residues, is an exceptional polymer for many encapsulation purposes due to its biocompatibility and mild ionic gelation conditions.<sup>11</sup> For example,

alginate has been used for encapsulation of cells for tissue engineering purposes<sup>12–15</sup> and has been investigated for the treatment of diabetes mellitus type I.<sup>16,17</sup> However, a number of technical barriers currently remain which limit the applicability of the  $\text{Ca}^{2+}$  induced gelation in microfluidics, including.<sup>18,19</sup> (1) Appropriate gelling conditions for micro-channels, (2) maintenance of good cell viability throughout encapsulation and post processing, (3) high throughput particle production, and (4) high throughput sorting of cell containing microparticles from empty ones. The latter limitation has largely been addressed by the development of sophisticated microfluidics cell-sorting systems.<sup>20,21</sup> Also, low throughput has recently been greatly enhanced with improved microfluidic device designs with highly multiplexed capacity for droplet generation<sup>22</sup> allowing about 1000 fold higher throughput than standard devices, which could also potentially be applied for synthesis of hydrogel microbeads. The remaining identified challenges on biocompatibility and microchannel compatible gelation are therefore the current main hurdles to this fledgling technology.

Recently, we reported a new approach for cell-friendly ionic crosslinking of ionotropic polymers which shows excellent features for solving both these limitations.<sup>23</sup> This method exploits the difference in equilibrium binding constants between anionic chelates and ionotropic polymers with inorganic cations. Selection of appropriate chelate and ion combinations in two different solutions allows for competitive ligand exchange between the chelates and ionotropic polymer upon mixing, which in turn can be tuned to control the kinetics of ionotropic induced gelation (Fig. 1a). For example, at pH 6.7, ZnEDDA–alginate solution will not gel, nor

<sup>a</sup> Biophysics and Medical Technology, Dept. of Physics, NTNU, Norwegian University of Science and Technology, NO-7491 Trondheim, Norway.

E-mail: [bjorn.stokke@ntnu.no](mailto:bjorn.stokke@ntnu.no)

<sup>b</sup> Department of Physics, School of Engineering and Applied Sciences (SEAS), Harvard University, Cambridge, Massachusetts 02138, USA

† Electronic supplementary information (ESI) available. See DOI: 10.1039/c6lc00769d

‡ These authors contributed equally to this work.

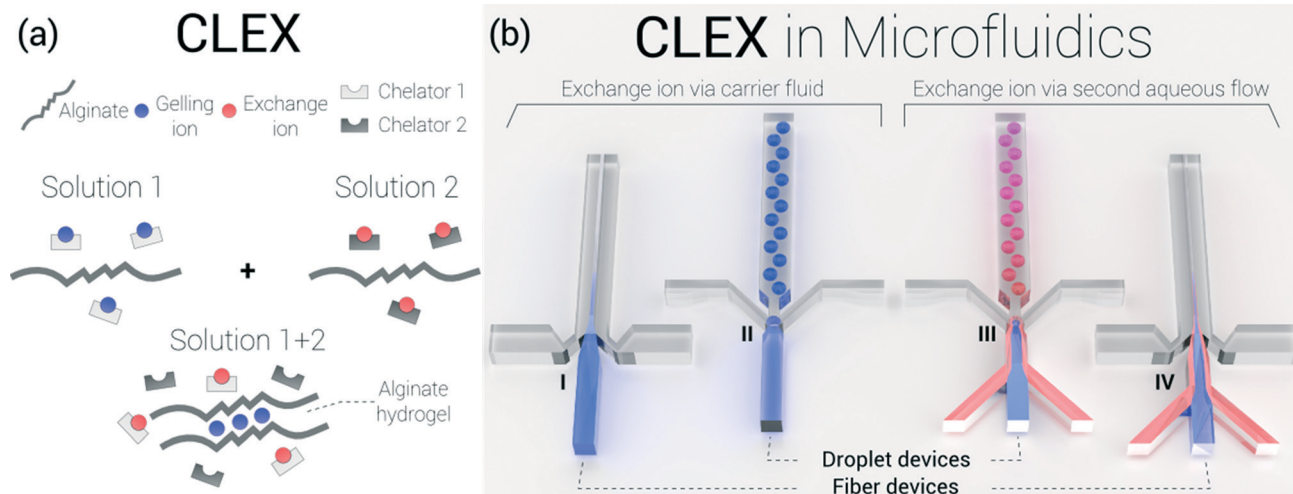


**Fig. 1** (a) Schematic illustration of CLEX (competitive ligand exchange crosslinking) mechanism for the synthesis of hydrogels from ionotropic polymers. The mechanism relies on competition between a gelling ion and an exchange ion towards two chelators and the ionotropic polymer (in this case alginate). One alginate solution containing a chelated gelling ion (solution 1) is mixed with another alginate solution containing a chelated exchange ion (solution 2) upon which the gelling ion is displaced by the exchange ion and rendered free to crosslink the alginate and form a hydrogel. (b) Illustration of microfluidic designs to apply the CLEX mechanism to form hydrogel microfibres (designs I and IV) and microbeads (designs II and III). Here, the chelated gelling and exchange ions are introduced individually via separate channels in the microfluidic device, either as a component of the aqueous flow and the carrier fluid (designs I and II) or via two aqueous flows (designs III and IV). The aqueous flows are coloured blue and red and the carrier fluid is grey. Upon contact of the separate flows containing the CLEX components the exchange ion will bind the gelling ion chelate and render the gelling ion free to crosslink the polymer solution.

will a CaEDTA–alginate solution, but upon mixing, the  $\text{Zn}^{2+}$  will be exchanged between EDDA and EDTA due to a difference in affinity, resulting in release of  $\text{Ca}^{2+}$  which subsequently cross-links the alginate. The kinetics and efficiency of this exchange process is dependent both on the pH and chelators used, allowing for control of both gel formation kinetics and gel strength through the amount of released cross-linking ions. Our approach, that we term competitive ligand exchange crosslinking (CLEX), is particularly interesting for applications in microfluidics as gelling is not instantaneous, but controlled from seconds to minutes by choice of chelates and pH of the precursor solutions which may be selected within the physiological range.<sup>23</sup> This temporal control of crosslinking kinetics is highly advantageous for microfluidic applications as this avoids problems of gelling at stagnation points within the microchannels associated with instantaneous gelling using free crosslinking ions. Moreover our initial findings have shown this approach to be highly compatible with a mammalian cell line and here we investigate this approach to encapsulate a wider variety of cell types and cultured over much longer durations.

The combined requirement of sufficient control of gelation and providing near physiological conditions for cells to be encapsulated within microfluidic channels is highly challenging. Here we demonstrate how CLEX can be utilized in co-flow microfluidic devices for the facile encapsulation of a variety of different cell types in alginate hydrogel microbeads and microfibers with high cell-viability and efficient device friendly gelation. We believe our approach to be advantageous over current commonly used gelling techniques since it overcomes several significant shortcomings; namely, the

need for a sheathing buffer solution to prolong diffusion of the gelling ion (which complicates design and operation),<sup>24</sup> the use of highly acidic conditions which is not suitable for certain prominent cell types (*i.e.* mammalian)<sup>25</sup> or solid components (*e.g.*  $\text{CaCO}_3$ ) suspended in the aqueous flow that will likely clog microchannels and prohibit synthesis of homogeneous gels.<sup>26</sup> In this study, we investigated the encapsulation of mammalian cells (pre-osteoblasts and Jurkat cells), a bacterium (*Synechocystis* sp. PCC 6803) and algae (*Chlamydomonas reinhardtii* CC-4532) and therefore focused on controlling the pH as appropriate for the various organism, all being in the range pH 6.0–8.0. Altering the pH of CLEX directly affects the kinetics of the gelation process and thus the gelation time, therefore a balance between suitable kinetics and cell friendly conditions was sought.

## Results and discussion

In order to apply the CLEX method to gel alginate within a microfluidic chip, a design which enables the mixing of an aqueous chelated gelling ion with an aqueous exchange ion solution at the point of droplet or fiber formation is needed to trigger the gelation reaction. This can be achieved by introducing the solutions containing the gelling and exchange ions in two separate flows that merge close to the droplet generating feature in the device. Some suitable designs are illustrated in Fig. 1b. Note that the microfluidic channel design should include an additional channel inlet for a second aqueous solution if the exchange ion cannot be introduced via the carrier fluid. As well as suitable chip design, it is essential to address the criteria of controlling gelation kinetics



and designing the process to be pH compatible with the immobilized cargo identified above.

### CLEX gelation of monodisperse alginate droplets

A hydrodynamic flow focusing device was fabricated to produce monodisperse Ca-alginate microbeads using CLEX (Fig. 1b III and 2).  $\text{Ca}^{2+}$  was used as the gelling ion and  $\text{Zn}^{2+}$  as the exchange ion since both these ions are well tolerated by humans.  $\text{Ca}^{2+}$  chelated with EDTA was mixed with the alginate precursor solution.  $\text{Zn}^{2+}$  chelated with EDDA was used as the exchange ion complex to release the  $\text{Ca}^{2+}$  from CaEDTA upon mixing and make this ion available to interact and induce gelation of the alginate. This combination was tested in the pH range of 6.0–8.0. Glycine was also investigated as a possible chelator for the  $\text{Zn}^{2+}$ , however, the gelation kinetics and therefore gelling was too rapid resulting in stagnation point gelation within the device (ESI† Fig. S1). This was the case even at higher pH (tested between pH 6.7 and 7.8) for the combination involving ZnGlycine. Fluorinated oil with biocompatible fluorosurfactant (similar to Holtze and co-workers<sup>27</sup>) was used as an immiscible carrier fluid to produce monodisperse emulsions of the precursor alginate solutions prior to gelation. This carrier fluid is biocompatible, offers high oxygen solubility<sup>28</sup> and is compatible with PDMS microchannels. Since we could find no zinc salt or  $\text{Zn}^{2+}$ -chelate combination that was soluble in this carrier fluid, an additional aqueous inlet was necessary to generate microbeads using CLEX (Fig. 1b, III). The microfluidic droplet device design therefore included three fluid inlets as illustrated in Fig. 2a; one inlet for the carrier fluid and two inlets for alginate solutions with chelated gelling ions (CaEDTA) and chelated exchange ions (ZnEDDA), respectively. Alginate was used in both solutions to balance the hydrodynamic resistance in the two channels and to avoid dilution of the final polymer concentration. Any fluctuations in hydrodynamic resistances resulting from polymer dilution would result in irregular device operation. Good hydraulic balance was achieved by introducing equal volumes of the two solutions in a co-flow region of the microfluidic channels prior to droplet break-up (Fig. 2b). The kinematic viscosity of the alginate solutions was found to be similar ( $22.1 \pm 0.4$  and  $21.3 \pm 0.1$  cSt for the alginate–CaEDTA and alginate–ZnEDDA solutions, respectively). Higher viscosity alginate solutions may cause irregular droplet formation.<sup>6</sup> We have previously shown that pH can alter the gelling kinetics of this system.<sup>23</sup> Here pH was adjusted to achieve a gelation time that was both be suitably long to avoid clogging of the channels, whilst also short enough to avoid droplet coalescence during collection. We found that a pH of 6.7 in both aqueous solutions gave a gelling time of  $9.0 \pm 3.5$  s and plateau storage modulus of  $420 \pm 13$  Pa (as measured by rheology, see ESI† Fig. S2) which was highly suitable for application in our microfluidic devices. Under these conditions no stagnation point gelation at the junction where the aqueous phases meet was observed and prolonged device operation (more

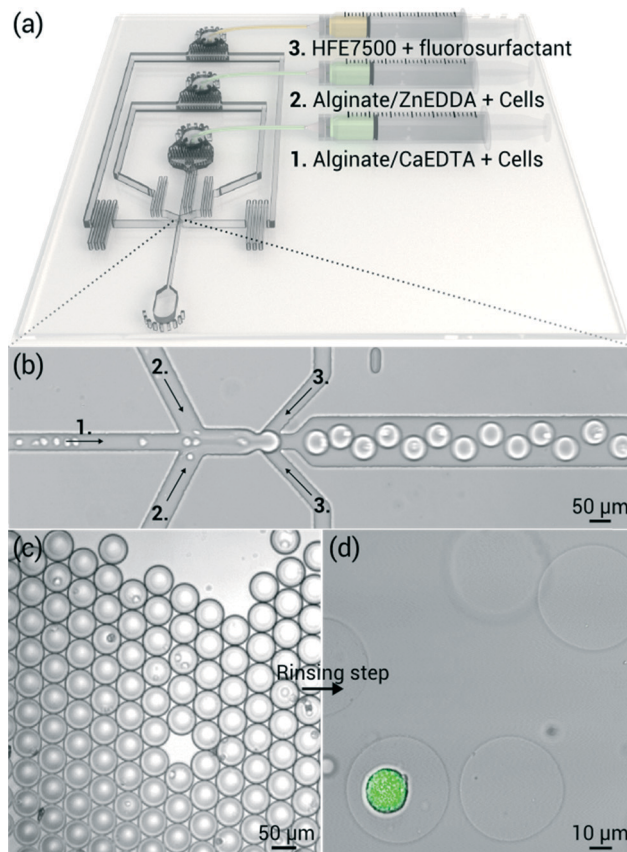


**Fig. 2** A droplet-based microfluidic device was used for encapsulation of cells in alginate microbeads with a new cell friendly and device compatible gelling mechanism. (a) A schematic of the microfluidic co-flow device. (b) Micrograph of the region of the device at which the encapsulation of cells occurs. (c) Micrograph of collected microgels suspended in the carrier oil with fluorosurfactant. (d) Confocal image of encapsulated pre-osteoblast cells in microgels after rinsing and re-suspending in cell medium to remove the oil and surfactant.

than 12 h) was achieved without evidence of droplet coalescence. The microbeads were produced at a frequency of 282 Hz with a mean diameter of  $53.2 \pm 1.0$  μm using flow rates of  $50 \mu\text{L h}^{-1}$  and  $200 \mu\text{L h}^{-1}$  for the two alginate solutions and the carrier fluid, respectively. At conditions of higher pH (above 7.2), the amount of  $\text{Ca}^{2+}$  for crosslinking of the alginate used in this study was insufficient to produce consistent microbeads since a competition between the alginate and EDDA for  $\text{Ca}^{2+}$  is shifted towards EDDA. As a result gelling was prolonged and we observed coalescence of precursor alginate droplets ~20–30 min after emulsification. We speculate that the alginate may alter the solubility of the hydrophilic surfactant tails (polyethylene glycol chains) resulting in reduced emulsion stability. Therefore, gelation should have proceeded sufficiently to prevent coalescence of emulsions before the surfactant becomes inefficient in stabilizing the droplets. In short, balance between gelation time and strength must be satisfied to effectively apply CLEX in microchannels, and this will vary with the type and concentration of ionotropic hydrogel, surfactant and carrier fluid used as

well as the dimensions and flow conditions of the microfluidic device.

pH has been shown to be of critical importance for cell metabolic activity and viability.<sup>29</sup> Contemporary alginate encapsulation methods that rely on a sudden drop in pH to release chelated  $\text{Ca}^{2+}$  therefore suffer from poor cell viability if cells are exposed to conditions of low pH for only a few minutes. We monitored conditions of pH during gelling using a fluorescent dye (*N*-(rhodamine 6G)-lactam-ethylenediamine (R6G-EDA)) and photon counting using a confocal microscope.<sup>30</sup> We compared the evolution of pH of CLEX alginate gel with an alginate containing CaEDTA and gelled by acetic acid contained in the oil phase as described by Utech and co-workers.<sup>24</sup> As expected, using ligand exchange, pH was maintained at a constant pH 6.7 for the duration of the experiment. However, in the case of CaEDTA containing alginate, which was initially adjusted to pH 6.7, upon addition of fluorinated oil containing acetic acid the pH rapidly dropped from pH 6.7 to pH 4.6 as  $\text{H}^+$  diffused from the oil phase to the aqueous alginate phase, a prerequisite to initiate gelling with this method (ESI† Fig. S3).

With CLEX, if the gelation kinetics are suitably slow, the alginate phases have time to properly mix. To illustrate this, we produced alginate microbeads with FITC labeled alginate

as one of the two dispersed components (Fig. 3a). Due to the slowed gelation kinetics with CLEX, the labeled alginate mixes with the second unlabeled alginate solution (Fig. 3b). In contrast, core-shell like microbeads are achieved due to very rapid gelling using an acidified carrier fluid (HFE7500 and acetic acid) which release  $\text{Ca}^{2+}$  from the CaEDTA almost instantly after a rapid pH drop (Fig. 3c). CLEX offers discrete control of the gelation time through choice of chelates and/or by adjusting the pH within physiological range of the precursor solutions, which opens possibilities of mixing the solutions on-chip using micro-mixers *e.g.* herringbone structures prior to droplet formation (slow gelation) or production of Janus and core-shell particles (quick gelation).

### CLEX for production of cell containing alginate microfibers

Reported methods for on-chip alginate microfiber production typically apply sheathing buffer solutions to delay diffusion of  $\text{Ca}^{2+}$  and thus gelation of alginate to avoid clogging of microchannels.<sup>31,32</sup> Since gelling kinetics can be tuned using ion chelate combinations and pH adjustment, CLEX is not reliant on delaying the flux of  $\text{Ca}^{2+}$  using a sheathing fluid and therefore chip design may be simplified. We propose a simplified route for facile on-chip fiber synthesis with only two aqueous components (one carrier fluid and one fluid with the ionotropic polymer) in a hydrodynamic flow focusing device (Fig. 4a and b). Here, dextran was used as the carrier fluid to match the viscosity of the alginate solution. The chelated exchange ion (ZnEDDA) was introduced *via* the carrier fluid (Fig. 1b, I). A 3D PDMS microfluidic device (Fig. 4a and b) was used which was fabricated using a previously reported method<sup>33</sup> to mimic glass capillary microfluidic devices often used for alginate fiber synthesis,<sup>15,34</sup> however, similar results could be achieved with standard 2D microfluidic devices using CLEX. The 3D junction offers coaxial flow focusing for the synthesis of axisymmetric fibers and a larger operation window of flow rate difference between the alginate and dextran solutions since the relatively large hydraulic resistance in the narrow region (Fig. 4a and b) channel restricts backflow of the carrier fluid.<sup>35</sup> Fabrication of coaxial flow focusing devices with cylindrical PDMS channels have previously been reported for the production of alginate fibers also using only two aqueous inlets (alginate and  $\text{CaCl}_2$ ),<sup>36</sup> however, the fabrication of such devices is cumbersome with existing lithography techniques. In our 3D device, CLEX was initiated upon contact between the alginate and dextran solutions where  $\text{Ca}^{2+}$  was gradually rendered free within the alginate containing solution to gel the alginate and form microfibers. For fiber production in microfluidic devices, it is necessary to initiate gelation before the fluid streams exit the device. Therefore, the choice of ions, chelates and pH as well as the flow rates are crucial parameters that need fine tuning for on-chip fiber synthesis. We found that the determined pH and ion-chelate combinations for droplet devices were also suitable for fiber synthesis with flow rates of  $200 \mu\text{L h}^{-1}$  and  $1000 \mu\text{L h}^{-1}$  for the alginate and

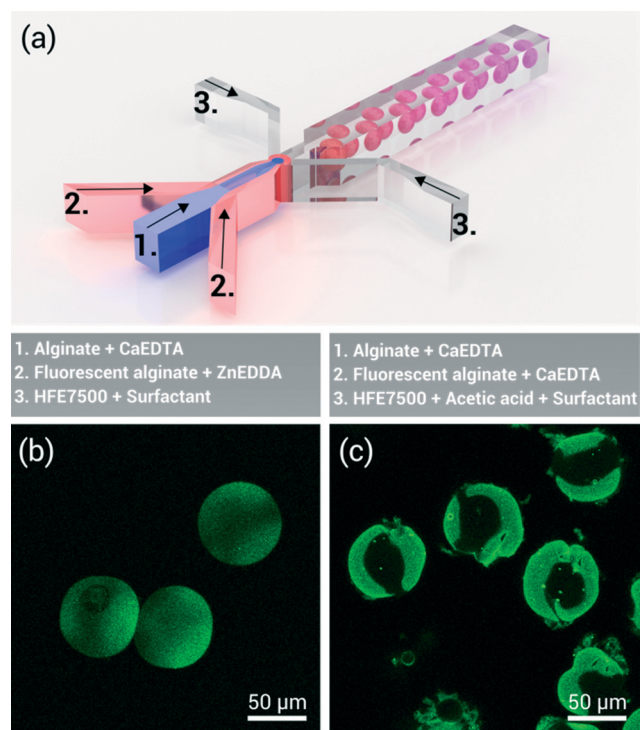


**Fig. 3** (a) The hydrodynamic flow focusing device used to encapsulate cells was also utilized to investigate the mixture of the two alginate solutions in the produced microbeads. This is the same device as in Fig. 1 III for which a micrograph is shown in Fig. 2b. (b) Using CLEX, the fluorescently labeled alginate was well distributed in the microbeads upon gradual release of  $\text{Ca}^{2+}$  from CaEDTA. (c) Release of  $\text{Ca}^{2+}$  from CaEDTA with an acidified carrier fluid initiated rapid gelation which yielded more distinct domains of fluorescently labeled and unlabeled alginate of the gelled microbeads.



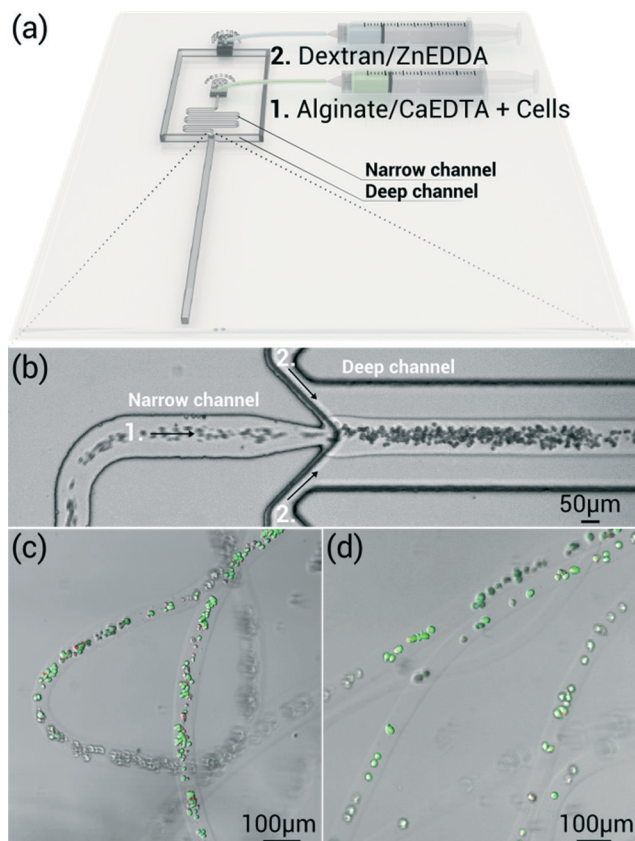


**Fig. 4** A microfluidics fiber device was used for the encapsulation of cells in alginate microfibers using CLEX. (a) A schematic of the 3D microfluidic fiber device. (b) Micrograph of the region of the device at which the two aqueous phases meet to form cell-laden alginate microfibers. (c) Confocal image of encapsulated Jurkat cells in microfibers suspended in cell medium. (d) Confocal image of encapsulated pre-osteoblasts in microfibers suspended in cell medium. No rinsing step is required as the continuous phase is aqueous.

dextran solutions, respectively. These parameters resulted in fibers with mean diameter of  $62.5 \pm 4.4 \mu\text{m}$  and a production rate of  $\sim 10 \text{ mm s}^{-1}$ . The fibers were collected immediately after production without intermediate rinsing steps (ESI† Fig. S4). We observed no stagnation point gelation, even after running the device for over 12 h. Cells were introduced into the alginate solution and were encapsulated in the microfibers. This approach enabled the formation of cell containing alginate microfibers directly into cell culture medium without a rinsing step. Two cell types were tested, non-adherent Jurkat cells (Fig. 4c) and adherent murine pre-osteoblasts (Fig. 4d) and excellent post encapsulation cell viability was observed for both cell types.

#### Cell viability in CLEX prepared alginate microbeads

Microfluidic encapsulation of various cell types in hydrogels including bacteria,<sup>37</sup> yeast<sup>38</sup> adherent and non-adherent mammalian cells<sup>39</sup> have previously been reported. However, difficulties in maintaining high cell viability rates throughout the encapsulation and subsequent gelling process have been

noted. The amount of encapsulated cells depends on the cell concentration and follows a Poisson distribution,<sup>40,41</sup> and we observed a similar behavior for all cells tested. Cells were injected *via* both aqueous phases in our two-alginate inlet droplet device to increase the encapsulation efficiency. Alginate samples containing cells were stirred continuously throughout the experiments to avoid sedimentation.

Successful encapsulation of highly viable bacteria, algae and mammalian cells in microbeads was achieved using our microfluidic design and gelling technique. We monitored the growth of the naturally fluorescent cyanobacteria *Synechocystis* sp. PCC 6803 and *Chlamydomonas reinhardtii* CC-4532 algae in the microgels until the cells formed colonies and escaped the microgel confinements (Fig. 5a and b, respectively). Using a standard live/dead staining assay after the collection and subsequent rinsing (Fig. 2c and d) of the hydrogels, high cell viability ( $\sim 95\%$ ) of the encapsulated mammalian pre-osteoblasts was achieved (Fig. 5c). The cells were monitored for 21 days with no significant change in cell viability. The alginate was not modified to facilitate cell adherence by, for example, functionalization with RGD-groups and we observe no cell division of the pre-osteoblasts within the hydrogels. Given the mild conditions of pH, the high viability of all the cell types tested is to be expected, however CLEX relies on high concentrations of potentially toxic ions such as  $\text{Zn}^{2+}$ .  $\text{Zn}^{2+}$  has been shown to be toxic for all the cell types tested: example  $\text{IC}_{50}$  values are 0.58, 8–16 and  $\sim 380 \mu\text{M}$  for *C. reinhardtii*,<sup>42</sup> *Synechocystis* sp.<sup>43</sup> and *MC3T3-E1* (ref. 44) cells respectively. Therefore it is highly interesting to note that no toxic effects were observed and this was likely due to all  $\text{Zn}^{2+}$  being strongly chelated throughout the CLEX reaction and therefore not biologically available to cause toxic effects.

#### Comparison with other gelation strategies

Forming a hydrogel of an ionotropic polymer, such as alginate, by crosslinking with a multivalent ion inside a microfluidic channel is a delicate process that is difficult to control on-chip since the rapid kinetics of gelation likely result in irregular droplet production or even complete clogging of the microchannels.<sup>24,25</sup> Introducing aqueous  $\text{Ca}^{2+}$  directly to the alginate stream in a device will result in immediate gelling and clogging of the channels. Therefore, in addition to having an inlet for  $\text{Ca}^{2+}$  and alginate, an extra inlet is often introduced to the microfluidic geometry whereby sheathing buffer is injected to temporarily shield the  $\text{Ca}^{2+}$  stream from the alginate.<sup>6,45,46</sup> The sheathing buffer acts as a barrier to delay diffusion of  $\text{Ca}^{2+}$  ions towards the alginate and therefore slows gelling. Currently, this is the standard approach for alginate fiber synthesis using microfluidic devices,<sup>31,32</sup> but has also been demonstrated for alginate bead synthesis.<sup>6</sup> The main drawback to this approach is inhomogeneous gelation and complexity in operating the microfluidic device due to the additional aqueous phase, and, if the  $\text{Ca}^{2+}$  solution temporarily comes in direct contact with the alginate stream, instant

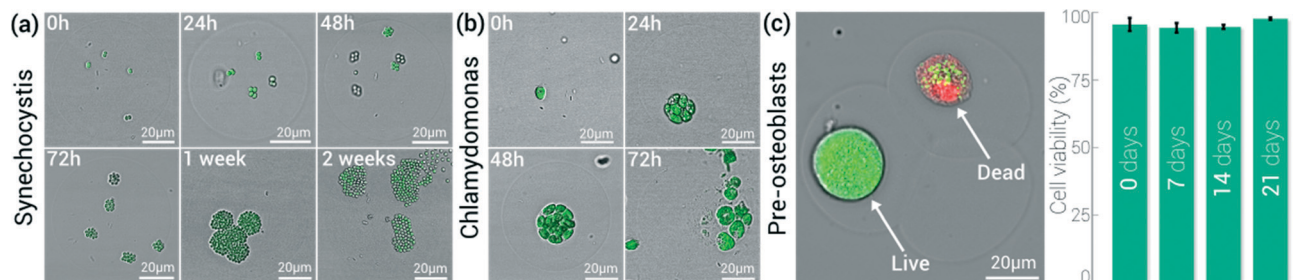


**Fig. 5** Micrographs of (a) the cyanobacteria *Synechocystis* sp. PCC 6803 and (b) of the algae *Chlamydomonas reinhardtii* CC-4532 encapsulated in alginate microbeads at indicated time points. After two weeks and 72 h the cyanobacteria and algae colonies grew beyond the microgel confinements, respectively. Images are overlaid images of bright field and fluorescent images capturing the auto fluorescence of chlorophyll produced by the bacteria and algae. (c) A live/dead staining assay was utilized to quantify the cell viability of microencapsulated pre-osteoblasts where live and dead cells appear green and red, respectively. The cell viability was monitored for 21 days after encapsulation showing high and constant survival rates (~95%). No cell division was observed.

gelation will take place, likely resulting in clogging. Others have opted to use oleic acid as the continuous phase as  $\text{CaCl}_2$  is partly soluble in this oil and will diffuse into the dispersed precursor alginate phase upon contact, resulting in gelation of the alginate downstream in the microfluidic device.<sup>19</sup> However, cell viability is strongly dependent on rapidly removing the oleic acid through an on-chip exchange mechanism with mineral oil introduced by an additional channel inlet.

In an attempt to overcome these shortcomings, pH sensitive  $\text{Ca}^{2+}$  chelates (e.g.  $\text{CaEDTA}$ ,  $\text{CaEGTA}$ ) or solid  $\text{CaCO}_3$  have been added to the dispersed phase with the alginate. To release the chelated  $\text{Ca}^{2+}$ , an acidified carrier fluid is typically applied to decrease the pH through the diffusion of  $\text{H}^+$  from the continuous to the dispersed phase resulting in subsequent internal gelation of the alginate.<sup>24,25,39,47–49</sup> Such approaches can be effective in achieving a slower and more homogeneous gelation that does not clog microfluidic channels immediately and result in well dispersed microparticles. However, all of these approaches are unfortunately reliant on reducing pH well below the physiological range and are therefore detrimental to many cell types. A recent study<sup>24</sup> showed that cell viability can be enhanced if the cell-loaded gels are rinsed from the acidic environment shortly after gelation, however, even after short time scales (~2 min), the survival rate of the encapsulated cells showed a decrease to ~80% and to ~0% after 30 min between encapsulation, gelation and re-suspension in cell medium. Also, surviving cells may show different metabolic behavior due to the stress induced by the temporary acidic environment. Encouraging results have been obtained by using solid  $\text{CaCO}_3$  in combination with glucono-1,5-lactone (GDL) in the carrier fluid to slowly release the  $\text{Ca}^{2+}$  in a milder fashion as compared to using an acidified carrier fluid.<sup>50</sup> However, the use of microcrystals or micron sized agglomerates of nanocrystals of  $\text{CaCO}_3$  as a gelling strategy can result in inhomogeneous gelation since the distribution of these particles will vary between droplets and the crystals may also cause clogging of narrow junctions in microfluidic devices.<sup>24,26</sup> Additionally, this gelation strategy is very slow (~hours), which makes the synthesis of more complex structures (e.g. core-shell or Janus parti-

cles) not possible since such structures require more rapid gelation. Others have explored the release of  $\text{Ca}^{2+}$  from photosensitive caged  $\text{Ca}^{2+}$  complexes,<sup>51</sup> but these chemical compounds, although offering a controlled release of  $\text{Ca}^{2+}$ , have limited appeal due to high costs and additional complexity.<sup>52</sup> Also, these approaches often rely on UV radiation which is detrimental to the structure of DNA and RNA if the dosage is high. The addition of short segments of oligoguluronates (OligoG's) to the alginate solutions represents an additional means to delay Ca-induced gelation and affect the final gel structure.<sup>53,54</sup> This strategy can be used in combination with the different methods to induce Ca-alginate gelation discussed above.

In contrast to previously used on-chip gelling techniques, CLEX allows gelling to occur at conditions of controlled pH. CLEX also offers precise control over gelation time and can therefore be tailored for various microfluidic applications requiring either slow (mixing of compounds) or quick (Janus and core-shell particle synthesis) gelation. An overview of alginate gelation strategies in microchannels with their perceived strengths and limitations is shown in Table 1.

## Experimental

### Preparation of precursor solutions

All chemicals were purchased from Sigma-Aldrich unless stated otherwise. All solutions were prepared using deionized water (DIW) with a resistivity of 15  $\text{M}\Omega\text{ cm}$  (Milli-Q™, Millipore). Alginate (source *L. hyperborea* stipe) with a guluronic acid residue fraction of  $F_G = 0.68$ , and a  $M_W$  of  $275 \times 10^3\text{ g mol}^{-1}$  (PROTANAL LF 2005) or  $F_G = 0.67$  and a  $M_W$  of  $275 \times 10^3\text{ g mol}^{-1}$  (PROTANAL SF 60) and labelled with Fluoresceinamine (both FMC Biopolymer, Haugesund, Norway) were dissolved in DIW to a final concentration of 3 wt/vol%. The fluorescently labelled alginate was made as described by Strand and coworkers.<sup>55</sup>  $\text{CaCl}_2$  was mixed with ethylenediaminetetraacetic acid (EDTA) and 3-(*N*-morpholino)propanesulfonic acid (MOPS) in aqueous solution and equal molar proportions and then adjusted to pH 6.7 using HCl and NaOH. This solution was then mixed with the

**Table 1** Overview of alginate gelation strategies that have been utilized in microfluidic systems with their strengths and weaknesses

	External	Internal			
(1) = Solution 1 (2) = Solution 2	(1) Alginate (2) CaCl <sub>2</sub>	(1) Alginate + CaEDTA/CaEGTA (2) Acetic acid	(1) Alginate + CaCO <sub>3</sub> (2) GDL	(1) Alginate + caged Ca <sup>2+</sup> UV-light	(1) Alginate + CaEDTA (2) Alginate/dextran + ZnEDDA
Cell viability	Excellent	Poor	Good <sup>a</sup>	Poor <sup>b</sup>	Excellent
Gelation in microchannels	None/poor <sup>c</sup>	Good <sup>d</sup>	Good	Excellent	Excellent
Choice of pH	Excellent	None	Good	Excellent	Excellent
pH stability during gelation	Excellent	None	Good <sup>e</sup>	Excellent	Excellent
Choice of gelation time	None	Poor	Poor	Poor <sup>f</sup>	Excellent
Gel homogeneity	Poor	Excellent	Good <sup>g</sup>	Excellent	Excellent
Price	Excellent	Excellent	Excellent	Poor	Excellent

<sup>a</sup> CO<sub>2</sub> as by-product upon release of Ca<sup>2+</sup>. <sup>b</sup> High UV dosage is detrimental to cells and may degrade biomolecules. <sup>c</sup> Requires shielding water stream. <sup>d</sup> Stagnation point gelation may occur due to rapid gel initiation. <sup>e</sup> Dependent on buffer solution. <sup>f</sup> Gelation is rapid when initiated. <sup>g</sup> Dependent on distribution of nano/micro agglomerates of CaCO<sub>3</sub> crystals.

alginate solution to give a final concentration of 0.6% (wt) alginate, 84 mM Ca<sup>2+</sup>, 84 mM EDTA, 40 mM MOPS. Zn(CH<sub>3</sub>CO<sub>2</sub>)<sub>2</sub> was mixed with ethylenediamine-*N,N'*-diacetic acid (EDDA) and 3-(*N*-morpholino)propanesulfonic acid (MOPS) in aqueous solution and then adjusted to pH 6.7 using HCl and NaOH. This solution was then mixed with the alginate solution to give a final concentration of 0.6% (wt) alginate, 84 mM Zn<sup>2+</sup>, 84 mM EDDA, 40 mM MOPS. In the case of fiber synthesis, the ZnEDDA was mixed with 8% (wt) dextran (source *Leuconostoc*, *M<sub>w</sub>*: 450 × 10<sup>3</sup>–650 × 10<sup>3</sup> g mol<sup>−1</sup>) instead of alginate.

### Rheology

The kinematic viscosity of 0.6 wt% alginate precursor solutions, prepared as described above at pH 6.7, was measured using a micro-Ubbelohde capillary viscometer (internal diameter 0.7 mm, Schott-Geräte GmbH, Germany). To determine the point of gelation and measure the modulus of the resulting gel, rheological characterisation was performed using a Paar Physica MCR 300 Rheometer as described previously.<sup>23</sup> Briefly, storage and loss moduli at a measuring gap of 1 mm were recorded as a function of time at an angular frequency ( $\omega$ ) of 1 rad s<sup>−1</sup>, amplitude of 1 mrad and temperature of 25 °C using a parallel plate geometry with serrated plate surfaces (PP50 serrated plate, diameter = 50 mm). Equal volumes (1.75 mL) of 2 component gels were measured onto the rheometer plate using a 5 mL pipette immediately prior to measurement. Gelation was determined to be the point at which the storage was equal to the loss modulus. All measurements were repeated a minimum of three times.

### Fabrication of microfluidic devices

PDMS microfluidic devices were molded from SU-8 masters. SU-8 3050 (MicroChem Corp.) was spun at 3000 RPM for 30 s onto a silicon wafer (University Wafers) and soft baked at 65 °C for 1 min and then 95 °C for 15 min. The resist was exposed with UV-light (250 mJ cm<sup>−2</sup>, 365 nm) using a

Süss MA-6 mask aligner through emulsion films (JD Photo-Tools, UK) with CAD designs of the microfluidic devices. The post-exposure bake was carried out at 65 °C for 1 min and then 95 °C for 5 min. The sample was developed for 5 min using a photoresist developer (mrDev 600, Micro Resist Technology). For the multilayered microfluidic devices that were utilized to synthesize alginate fibers, the above steps were repeated for a second layer of photoresist and UV exposer through a second emulsion film to render 3D structures. Two-component Sylgard® 184 PDMS (Dow Corning) (10:1) was mixed, degassed in a desiccator, poured over the SU-8 mold and baked for 3 hours at 65 °C. The cured PDMS was peeled from the mold and inlets were made using a punch (Ø 1 mm, UniCore). The feature side of the PDMS was treated with oxygen plasma (Femto plasma cleaner) and bonded to a flat slab of PDMS. For the droplet devices, the PDMS devices were rendered fluorophilic prior to use by filling with hydrofluoroether (HFE7500, 3M) containing 2% (v/v) fluorosilane (1H,1H,2H,2H-perfluorooctyl) to increase the oil wetting. The oil was removed by blow drying with a N<sub>2</sub>-gun. No surface treatment was carried out prior to use of the fiber devices.

### Cell culture

Murine calvarial pre-osteoblast cells, MC3T3-E1 subclone 4 (ATCC® CRL-2593™) were cultured to 80% confluence in  $\alpha$ -MEM supplemented with 1  $\mu$ M ml<sup>−1</sup> gentamicin, 2 mM glutamine and 10% foetal calf serum. Cells were detached using trypsin/EDTA, suspended in PBS, and centrifuged at 1500 RPM. Cells were re-suspended in fresh culture medium prior to mixing with alginate solutions.

Human T lymphocyte cells (Jurkat, clone E6-1, ATCC® TIB-152™) were cultured in RPMI-1640 medium supplemented with 10% foetal calf serum, 2 mM glutamine, sodium pyruvate and 1  $\mu$ M ml<sup>−1</sup> gentamicin.

*Synechocystis* sp. PCC 6803 cells were grown in 200 ml of BG 11 media<sup>56</sup> with 5 mM glucose at 30 °C under continuous



illumination ( $20 \mu\text{E m}^{-2} \text{s}^{-1}$ ) for 72 hours before encapsulation.

The alga *Chlamydomonas reinhardtii* CC-4532 was grown in TAP medium<sup>57</sup> at 18 °C under continuous illumination (light intensity:  $20 \mu\text{E m}^{-2} \text{s}^{-1}$ ) for 72 hours before encapsulation.

### Cell encapsulation in alginate microbeads and microfibers

HFE7500 (3M®), a low viscosity hydrofluoroether that offers high gas transport and avoids swelling of PDMS devices, was used as the continuous phase. Fluorinated surfactant containing two oligomeric perfluorinated polyethers (Krytox® FSH 157, DuPont) attached to polyethyleneglycol (ED-900 Jeffamine®, Huntsman) was kindly provided by Gianluca Etienne from the Soft Materials Laboratory (SMaL, EPFL). The synthesis follows a previously described procedure by Holtze and coworkers.<sup>27</sup> 2% (wt) of this fluorosurfactant was added to the continuous phase to facilitate droplet breakup and stabilize precursor alginate emulsions to avoid coalescence prior to gelation. Two dispersed phases were used: (1) 0.6% (wt) alginate containing 84 mM CaEDTA and 40 mM MOPS at pH 6.7 with cells and (2) 0.6% (wt) alginate containing 84 mM ZnEDDA and 40 mM MOPS at pH 6.7 with cells (Fig. 2a). The two dispersed phases meet in a co-flow region in the microfluidic channels prior to droplet break-up. The flow rates were set to  $200 \mu\text{L h}^{-1}$  for the continuous phase and  $50 \mu\text{L h}^{-1}$  for both dispersed phases by controlled injection using BD plastic syringes with PE plastic tubes (Scientific Commodities Inc.) mounted on syringe pumps (Harvard Apparatus, PHD ULTRA). The syringes used for the dispersed phases contained magnets and were stirred continuously to avoid sedimentation of cells. We injected cells *via* both dispersed phases to increase the encapsulation efficiency.

The cell-laden gels were collected directly in the appropriate cell medium and rinsed using 20% (v/v) PFO (1H,1H,2H,2H-perfluoro-1-octanol) for surfactant removal and centrifuged at 2500 rpm for 2 min to remove the HFE7500, fluorosurfactant and PFO by phase separation. The gels were collected in  $\alpha$ MED culturing medium for the pre-osteoblast and Jurkat cells, BG11-medium for the *Synechocystis* sp. PCC 6803 and TAP-medium for the *Chlamydomonas reinhardtii* CC-4532. The encapsulated *Synechocystis* and *Chlamydomonas* were kept at 30 °C and 18 °C respectively, at constant illumination and with slight agitation between imaging to ensure optimal culturing conditions. The encapsulated pre osteoblasts and Jurkat cells were incubated in  $\alpha$ MED at 37 °C.

To assess cell viability post encapsulation a calcein-AM/ethidium homodimer-1 assay (LIVE/DEAD® Viability/Cytotoxicity Kit, L-3224, Molecular Probes®) was applied. The cell-loaded alginate gels were imaged using a Leica SP5 confocal microscope.

The microfluidic device used for controlled synthesis of cell-laden alginate microfibers is shown in Fig. 4a and b. Unlike the droplet based device, an immiscible carrier fluid was

not applied as we aimed to produce continuous fibers. We used two aqueous phases for the facile production of alginate fiber: (1) 8% dextran with 84 mM ZnEDDA and 40 mM MOPS at pH 6.7 as the continuous phase and (2) 0.6% (wt) alginate containing 84 mM CaEDTA and 40 mM MOPS at pH 6.7 with cells as the inner phase. We utilized a 3D PDMS–PDMS device to mimic the glass capillary device often used for alginate fiber production.<sup>34</sup> The cell-laden fibers were collected directly in the appropriate cell medium by slicing the PDMS chip at the outlet and suspending it directly in the medium. The fiber-encapsulated cells were stored in appropriate conditions dependent on cell type as stated above. The same live/dead assay was used to assess the cell viability within the alginate microfibers.

## Conclusions

In recent years microfluidics has emerged as a powerful tool for the encapsulation and manipulation of cells in microgels. This has particular relevance for tissue engineering applications as a route to create biopolymer based hydrogel scaffolds to mimic the extracellular matrix in terms of both structural and biochemical features. Due to excellent biocompatibility and relatively mild gelling conditions, alginate is often applied for these purposes. Although interest and activity in the field of microencapsulation of cells in alginate hydrogels continues to grow, the lack of viable cell compatible and micro-channel friendly alginate crosslinking methods has stagnated progress in this area. To date the most reliable approach has been to apply an acidified carrier fluid that lowers the pH of the aqueous flow to release a divalent ion (typically  $\text{Ca}^{2+}$ ) from a pH sensitive chelate. Although offering homogenous and well controlled gelation, this approach is often not suitable for many cell types since a reduction in pH below that of natural conditions is detrimental to cell viability. Here, we demonstrate a route to achieve cell friendly, pH stable and microfluidic compatible cell encapsulation in alginate microbeads and microfibers. This was achieved by applying a newly developed method to control the availability of a crosslinking ion to a polymeric network *via* competitive ligand exchange, recently described by our group. The resulting cell-laden microgels were homogenous, monodisperse and demonstrated excellent cytocompatibility with a variety of cell types.

## Acknowledgements

The authors thank the Norwegian Micro- and Nano-Fabrication Facility, NorFab for financial support to AGH, JMR and BTS the Research Council of Norway for their support to DCB and PS through the FRINATEK program (project 214607). The work at Harvard was supported by the NSF (DMR-1310266) and the Harvard MRSEC (DMR-1420570). The authors would like to thank Gianluca Etienne and Prof. Esther Amstad (Soft Materials Laboratory, EPFL, Lausanne, Switzerland) for kindly providing the biocompatible fluorosurfactant used in this work. We would also like to thank Mr.

Jacob Joseph Lamb for providing the *Synechocystis*, Gunvor Røkke for providing the *Chlamydomonas* and Prof. Berit Løkensgard Strand (NTNU, Dept. of Biotechnology, Trondheim, Norway) for the generous donation of alginate samples used thorough in this work. The authors would also like to thank Sindre Bjørnøy (NTNU, Dept. of Physics, Trondheim, Norway) for his invaluable assistance in using a flow cell for pH monitoring of gelation and analysis of obtained data. Lastly, we thank the NTNU Nanolab for providing a state-of-the-art cleanroom facility for microfluidic chip fabrication.

## References

- 1 M. O. Olderoy, M. Xie, J.-P. Andreassen, B. L. Strand, Z. Zhang and P. Sikorski, *J. Mater. Sci.: Mater. Med.*, 2012, **23**, 1619–1627.
- 2 M. O. Olderoy, M. Xie, B. L. Strand, E. M. Flaten, P. Sikorski and J.-P. Andreassen, *Cryst. Growth Des.*, 2009, **9**, 5176–5183.
- 3 M. K. Li and H. S. Fogler, *J. Fluid Mech.*, 1978, **88**, 499–511.
- 4 S. Sugiura, T. Oda, Y. Izumida, Y. Aoyagi, M. Satake, A. Ochiai, N. Ohkohchi and M. Nakajima, *Biomaterials*, 2005, **26**, 3327–3331.
- 5 S. Sugiura, T. Oda, Y. Aoyagi, R. Matsuo, T. Enomoto, K. Matsumoto, T. Nakamura, M. Satake, A. Ochiai, N. Ohkohchi and M. Nakajima, *Biomed. Microdevices*, 2007, **9**, 91–99.
- 6 L. Mazutis, R. Vasiliauskas and D. A. Weitz, *Macromol. Biosci.*, 2015, **15**, 1641–1646.
- 7 W. R. Gombotz and S. F. Wee, *Adv. Drug Delivery Rev.*, 2012, **64**, 194–205.
- 8 A. Kang, J. Park, J. Ju, G. S. Jeong and S.-H. Lee, *Biomaterials*, 2014, **35**, 2651–2663.
- 9 H. Geckil, F. Xu, X. H. Zhang, S. Moon and U. Demirci, *Nanomedicine*, 2010, **5**, 469–484.
- 10 X. T. Sun, M. Liu and Z. R. Xu, *Talanta*, 2014, **121**, 163–177.
- 11 T. A. Becker, D. R. Kipke and T. Brandon, *J. Biomed. Mater. Res.*, 2001, **54**, 76–86.
- 12 C.-C. Wang, K.-C. Yang, K.-H. Lin, H.-C. Liu and F.-H. Lin, *Biomaterials*, 2011, **32**, 7118–7126.
- 13 K. H. Lee, S. J. Shin, Y. Park and S.-H. Lee, *Small*, 2009, **5**, 1264–1268.
- 14 M. Xie, M. O. Olderoy, J.-P. Andreassen, S. M. Selbach, B. L. Strand and P. Sikorski, *Acta Biomater.*, 2010, **6**, 3665–3675.
- 15 H. Onoe, T. Okitsu, A. Itou, M. Kato-Negishi, R. Gojo, D. Kiriya, K. Sato, S. Miura, S. Iwanaga, K. Kuribayashi-Shigetomi, Y. T. Matsunaga, Y. Shimoyama and S. Takeuchi, *Nat. Mater.*, 2013, **12**, 584–590.
- 16 O. Veisoh, J. C. Doloff, M. Ma, A. J. Vegas, H. H. Tam, A. R. Bader, J. Li, E. Langan, J. Wyckoff, W. S. Loo, S. Jhunjunwala, A. Chiu, S. Siebert, K. Tang, J. Hollister-Lock, S. Aresta-Dasilva, M. Bochenek, J. Mendoza-Elias, Y. Wang, M. Qi, D. M. Lavin, M. Chen, N. Dholakia, R. Thakrar, I. Lacik, G. C. Weir, J. Oberholzer, D. L. Greiner, R. Langer and D. G. Anderson, *Nat. Mater.*, 2015, **14**, 643–652.
- 17 P. Soonshiong, E. Feldman, R. Nelson, R. Heintz, Q. Yao, Z. W. Yao, T. L. Zheng, N. Merideth, G. Skjakbraek, T. Espevik, O. Smidsrod and P. Sandford, *Proc. Natl. Acad. Sci. U. S. A.*, 1993, **90**, 5843–5847.
- 18 E. Tumarkin and E. Kumacheva, *Chem. Soc. Rev.*, 2009, **38**, 2161–2168.
- 19 C. Kim, K. S. Lee, Y. E. Kim, K.-J. Lee, S. H. Lee, T. S. Kim and J. Y. Kang, *Lab Chip*, 2009, **9**, 1294–1297.
- 20 J.-C. Baret, O. J. Miller, V. Taly, M. Ryckelynck, A. El-Harrak, L. Frenz, C. Rick, M. L. Samuels, J. B. Hutchison, J. J. Agresti, D. R. Link, D. A. Weitz and A. D. Griffiths, *Lab Chip*, 2009, **9**, 1850–1858.
- 21 J. Nam, H. Lim, C. Kim, J. Y. Kang and S. Shin, *Biomicrofluidics*, 2012, **6**, 024120.
- 22 H.-H. Jeong, V. R. Yelleswarapu, S. Yadavali, D. Issadore and D. Lee, *Lab Chip*, 2015, **15**, 4387–4392.
- 23 D. C. Bassett, A. G. Håti, T. B. Melø, B. T. Stokke and P. Sikorski, *J. Mater. Chem. B*, 2016, DOI: 10.1039/C6TB01812B.
- 24 S. Utech, R. Prodanovic, A. S. Mao, R. Ostafe, D. J. Mooney and D. A. Weitz, *Adv. Healthcare Mater.*, 2015, **4**, 1628–1633.
- 25 V. L. Workman, S. B. Dunnett, P. Kille and D. D. Palmer, *Biomicrofluidics*, 2007, **1**.
- 26 H. Zhang, E. Tumarkin, R. M. A. Sullan, G. C. Walker and E. Kumacheva, *Macromol. Rapid Commun.*, 2007, **28**, 527–538.
- 27 C. Holtze, A. C. Rowat, J. J. Agresti, J. B. Hutchison, F. E. Angile, C. H. J. Schmitz, S. Koster, H. Duan, K. J. Humphry, R. A. Scanga, J. S. Johnson, D. Pisignano and D. A. Weitz, *Lab Chip*, 2008, **8**, 1632–1639.
- 28 J. G. Riess and M. P. Krafft, *Artif. Cells, Blood Substitutes, Immobilization Biotechnol.*, 1997, **25**, 43–52.
- 29 A. Kurkdjian and J. Guern, *Annu. Rev. Plant Physiol. Plant Mol. Biol.*, 1989, **40**, 271–303.
- 30 S. Bjørnøy, S. Mandaric, D. Bassett, A. Åslund, S. Ucar, J. Andreassen, B. Strand and P. Sikorski, *Acta Biomater.*, 2016, DOI: 10.1016/j.actbio.2016.07.046.
- 31 M. Yamada, S. Sugaya, Y. Naganuma and M. Seki, *Soft Matter*, 2012, **8**, 3122–3130.
- 32 C. Martino, C. Statzer, D. Vigolo and A. J. deMello, *Lab Chip*, 2016, **16**, 59–64.
- 33 A. Rotem, A. R. Abate, A. S. Utada, V. Van Steijn and D. A. Weitz, *Lab Chip*, 2012, **12**, 4263–4268.
- 34 S. Shin, J.-Y. Park, J.-Y. Lee, H. Park, Y.-D. Park, K.-B. Lee, C.-M. Whang and S.-H. Lee, *Langmuir*, 2007, **23**, 9104–9108.
- 35 W.-C. Jeong, J.-M. Lim, J.-H. Choi, J.-H. Kim, Y.-J. Lee, S.-H. Kim, G. Lee, J.-D. Kim, G.-R. Yi and S.-M. Yang, *Lab Chip*, 2012, **12**, 1446–1453.
- 36 E. Kang, S.-J. Shin, K. H. Lee and S.-H. Lee, *Lab Chip*, 2010, **10**, 1856–1861.
- 37 Y.-J. Eun, A. S. Utada, M. F. Copeland, S. Takeuchi and D. B. Weibel, *ACS Chem. Biol.*, 2011, **6**, 260–266.
- 38 C.-H. Choi, J.-H. Jung, Y. W. Rhee, D.-P. Kim, S.-E. Shim and C.-S. Lee, *Biomed. Microdevices*, 2007, **9**, 855–862.
- 39 W. H. Tan and S. Takeuchi, *Adv. Mater.*, 2007, **19**, 2696–2701.
- 40 S. Koester, F. E. Angile, H. Duan, J. J. Agresti, A. Wintner, C. Schmitz, A. C. Rowat, C. A. Merten, D. Pisignano, A. D. Griffiths and D. A. Weitz, *Lab Chip*, 2008, **8**, 1110–1115.
- 41 D. J. Collins, A. Neild, A. deMello, A.-Q. Liu and Y. Ai, *Lab Chip*, 2015, **15**, 3439–3459.

- 42 P. Mikulic and J. Beardall, *Chemosphere*, 2014, **112**, 402–411.
- 43 B. Blasi, L. Peca, I. Vass and P. B. Kos, *J. Microbiol. Biotechnol.*, 2012, **22**, 166–169.
- 44 S. B. Delia, G. Eileen, F. F. David, M. S. Molly and G. H. Robert, *Biomed. Mater.*, 2011, **6**, 045007.
- 45 J. Xu, S. Li, J. Tan and G. Luo, *Chem. Eng. Technol.*, 2008, **31**, 1223–1226.
- 46 Y. Jun, E. Kang, S. Chae and S.-H. Lee, *Lab Chip*, 2014, **14**, 2145–2160.
- 47 S. Akbari and T. Pirbodaghi, *Microfluid. Nanofluid.*, 2013, **16**, 773–777.
- 48 M. Marquis, V. Alix, I. Capron, S. Cuenot and A. Zykwinska, *ACS Biomater. Sci. Eng.*, 2016, **2**, 535–543.
- 49 Q. Chen, S. Utech, D. Chen, R. Prodanovic, J.-M. Lin and D. A. Weitz, *Lab Chip*, 2016, **16**, 1346–1349.
- 50 Y. Morimoto, W.-H. Tan, Y. Tsuda and S. Takeuchi, *Lab Chip*, 2009, **9**, 2217–2223.
- 51 J. Cui, M. Wang, Y. Zheng, G. M. Rodriguez Muniz and A. del Campo, *Biomacromolecules*, 2013, **14**, 1251–1256.
- 52 B.-H. Chueh, Y. Zheng, Y.-S. Torisawa, A. Y. Hsiao, C. Ge, S. Hsiong, N. Huebsch, R. Franceschi, D. J. Mooney and S. Takayama, *Biomed. Microdevices*, 2010, **12**, 145–151.
- 53 T. E. Jorgensen, M. Sletmoen, K. I. Draget and B. T. Stokke, *Biomacromolecules*, 2007, **8**, 2388–2397.
- 54 H. Liao, W. Ai, K. Zhang, M. Nakauma, T. Funami, Y. Fang, K. Nishinari, K. I. Draget and G. O. Phillips, *Polymer*, 2015, **74**, 166–175.
- 55 B. L. Strand, Y. A. Morch, K. R. Syvertsen, T. Espevik and G. Skjak-Braek, *J. Biomed. Mater. Res., Part A*, 2003, **64**, 540–550.
- 56 J. J. Eaton-Rye, in *Photosynthesis Research Protocols*, ed. R. Carpentier, 2nd edn, 2011, vol. 684, pp. 295–312.
- 57 D. S. Gorman and R. P. Levine, *Proc. Natl. Acad. Sci. U. S. A.*, 1965, **54**, 1665–1669.